

Evaluation of titanium alloy as heat absorber for solar-based water treatment system

Nattadon Pannucharoenwong^{a,*}, Phadungsak Rattanadecho^a, Snunkhaem Echaroj^a,
Suwipong Hemathulin^b, Chatchai Benjapiyaporn^c, Kriengkrai Nabudda^c

^a Center of Excellence in Electromagnetic Energy Utilization in Engineering (CEEE), Department of Mechanical Engineering, Thammasat University, Pathumthani, 12120, Thailand

^b Department of Mechanical and Industrial, Rajabhat Sakon Nakhon University, Sakon Nakhon 47000, Thailand

^c Department of Mechanical Engineering, Khon Kaen University, Khon Kaen 40000, Thailand

Received 13 July 2021; accepted 27 July 2021

Abstract

Due to the current status of water treatment system it is very difficult to produce fresh clean water without electricity. This research evaluated the intervention of titanium as heat absorber in the heat transfer analysis regarding the solar-based desalination system. The experiment was carried out in a double-slanted distillation unit designed to harness sunlight's energy. The distillation unit contain a transparent glass shield, contaminated water inlet, treated water outlet, two treatment levels, heat absorber and insulator. Parameters monitors during the experiments included water treatment efficiency, productivity, distillation temperature and distillation rate. Variable included the heat absorber's surface area with respect to the surface area of water in the chamber (10 to 90%). Experimental results were used to calculate water treatment efficiency using the Engineering Equation Solver (EES), which varied disproportionally with the size of Titanium heat absorber. The highest productivity was observed at 1.61 liter per day with a water treatment efficiency of 26.2%. The payback period of the solar-based distillation prototype was 5.5 years. The fastest distillation rate was monitored at 15:00 on average. Water's level in distillation chamber and thermal conductivity of the insulator's thermal conductivity inside both lower and higher still inside the unit have undesirable impact on performance. Wind speed promoted better heat transfer which resulted in an increase in distillation rate. Two numerical equations were developed for calculating distillation efficiency and productivity from input parameters such as operating time and heat absorber's size. The prototype distillation unit demonstrated excellent results for converting salt water into fresh water. © 2021 The Author(s). Published by Elsevier Ltd. This is an open access article under the CC BY-NC-ND license (<http://creativecommons.org/licenses/by-nc-nd/4.0/>).

Peer-review under responsibility of the scientific committee of the Tmrees, EURACA, 2021.

Keywords: Distillation rate; Solar-base technology; Heat absorber; Titanium; Solar radiation

* Corresponding author.

E-mail address: pnattado@engr.tu.ac.th (N. Pannucharoenwong).

<https://doi.org/10.1016/j.egy.2021.07.082>

2352-4847/© 2021 The Author(s). Published by Elsevier Ltd. This is an open access article under the CC BY-NC-ND license (<http://creativecommons.org/licenses/by-nc-nd/4.0/>).

Peer-review under responsibility of the scientific committee of the Tmrees, EURACA, 2021.

Nomenclature

m_{gla}	Glass screen weight, kg
m_{insul}	Insulator weight, kg
$C_{\text{p,gla}}$	Heat capacity for glass material, J/kg °C
$C_{\text{p,H}_2\text{O}}$	Heat capacity for water, J/kg °C
ε_{g}	Glass emissivity
ε_{w}	Water emissivity
a_{g}	Radiation absorbed by the glass screen
a_{w}	Radiation absorbed
ρ_{g}	Glass reflectivity, kg/cm ³
U_{h}	Overall heat transfer coefficient, W/m ² K
T_{insul}	Temperature for the insulator, °C
$T_{\text{gla.2}}$	Temperature for the glass screen in the bottom layer, °C
$T_{\text{gla.1}}$	Temperature for the glass screen in the upper layer, °C
$T_{\text{H}_2\text{O.2}}$	Temperature for water surface in the bottom layer, °C
$T_{\text{H}_2\text{O.1}}$	Temperature for water surface in the upper layer, °C

1. Introduction

Fresh water is necessary especially during a pandemic virus outbreak such as the current Coronavirus disease (COVID-19) crisis. World Health Organization reported that the lethal COVID-19 while having fragile membrane can have survived as long as 2 days in dechlorinated tap water, hospital and domestic sewage [1,2]. Since most current water treatment system rely on electricity, water contamination is a major problem for rural areas that do not have access to electricity [3]. Additionally, since salt water is abundant and can be acquired in many areas in Thailand, water treatment system can also be applying to transform salt water into clean water. It is therefore useful for all communities to have a water treatment system that do not rely on electricity. Solar-based water treatment system can be adapting in rural area to convert salt water to clean water with very little or no electricity consumption.

The amount of solar radiation in Thailand have been observed through various different systems. Solar radiation data was found to correlate linearly with cloud cover data measured in 24 sites in Thailand [4]. Statistical analysis of collected data revealed mean solar radiation in the South of Thailand to be 450 w/m² [5]. Another study employed the Solargis model to estimate daily maximum global horizontal radiation (GHI) of different areas in Thailand. Daily solar radiation was found to be most intense in the Eastern (5.4 kWh/m²) and Central (5.1 kWh/m²) part of Thailand [6]. Due to current development in digital signal transmission system, a more precise solar tracking system can be employed. Chaowanan Jamroen et al. reported the usage of a low-cost automatic dual-axis solar tracking system, which was found consume half of the energy required for normal solar tracking system [7]. These innovation results in a better system for evaluating the effectiveness of solar-base device. So far many solar-based distillation units have been employed for producing clean water from contaminated water [8,9].

Solar-based desalination system usually employed heat transfer mechanism to promote distillation of high salt concentrated solution in a distillation chamber There are currently two different types of solar-based distillation system; passive and active type. Active distillation unit comprised of an external source of energy that required electricity input to operate effectively [10]. For instance, Hosseini et al. developed an active distillation unit for water treatment assisted by a vacuum heat exchanger which was capable of producing 1.5 kg of clean water per m² per day [11]. Although active distillation unit are relatively effective, it is still difficult to construct and implement this type of water treatment system in rural area. Passive type of distillation unit does not use electricity to operate, so water treatment activity is initialed and carried out entirely by radiation from sunlight [12,13]. A generic form of passive distillation unit for water treatment consisted of two slanted chamber for carrying contaminated water, an inlet/outlet, transparent glass shield, heat absorbers and insulator. Different operating conditions were observed to influence the distillation performance such as material used to make the heat absorber, water height inside the chamber, wind speed, and angle of the slanted slope. Optimization of water treatment process using solar-based

distillation unit were studied by many researches. Arash Ranjbaran and Mahdi Norozi prototyped a hybrid solar distillation unit with parabolic trough collector and cascading solar still capable of recycling 6 kg/m² of brine solution. In this research a cascading type still was observed to perform significantly better compared with a single basin still [14]. Ravishankar Sathyamurthy et al. proposed usage of sand cube as heat absorber to facilitate efficient heat transfer inside a solar-based water treatment system [15]. Different types of heat absorbers have been employed to improve the performance of the distillation unit. For instance, addition of charcoal heat absorber to a V-configuration distillation unit with advance sunlight collector system was found to increase efficiency to 30% [16]. A parabolic type solar-based distillation system was also employed for extraction of volatile oil [17]. Additionally, the solar technology was applied for absorption cooling system which provided both clean water and atmospheric cooling of the system [18].

2. Development of heat profile inside the system

Radiation from sunlight travel from the atmosphere into contaminated water inside two sloped chambers. Heat is initially absorbed and penetrated through the transparent glass shield in the upper chamber. The penetrated heat was absorbed by the contaminated water causing molecular vibration. Eventually, the accumulated energy exceeds the threshold energy which cause the intermolecular bond to break and evaporation of water. Water vapor will rise toward the transparent glass shield and then condensed back to liquid form which will fall onto a metal gutter on top of the chamber. The gutter is slightly slope to allow treated water to fall into a collector at the bottom.

2.1. Estimation of insolation using radiation ratio equation

Calculation of solar energy that reaches the Earth’s surface is referred to as insolation. Unlike solar radiation solar insolation is affected by angle of sun and distance from the sun, and atmosphere. For this reason, insolation varies significant due to differences in the measurement position, time of the day and month of the year. For this reason, insolation needed to be recorded throughout the year in order to determinate the highest average solar radiation. A generic equation for calculating insolation is shown in Eq. (1). Solar insolation (S_{IH}) is determined as the product between solar insolation per day (S_{ID}) and the total daily radiation ratio (DR_{ratio}) is shown in Eq. (2).

$$S_{IH} = S_{ID} \times DR_{ratio} \tag{1}$$

$$DR_{Total} = \pi \left(\frac{a + b \cos \omega}{24} \right) \times \frac{\cos \omega - \cos \omega_s}{\sin \omega_s - \left(\frac{2\pi \omega_s}{360} \right) \cos \omega_s} \tag{2}$$

$$a = a_1 + a_2 \sin \sin (\omega_s - 60) \text{ and } b = b_1 + b_2 \sin \sin (\omega_s - 60)$$

The incidence angle between sunlight and collided platform is denoted as ω_s , a and b values are constants that are determine by the measurement location. Since this experiment was performed in Kalasin province the coefficient values are used according to reference ($a_1 = 0.79$, $a_2 = -0.033$, $b_1 = 0.202$ and $b_2 = 0.218$).

2.2. Energy balance inside the solar-based system

Heat transfer analysis is an important step in determining possible heat loss inside the distillation unit system. Convective and radiation heat transfer are usually responsible for heat transfer from air to either liquid or solid material. However, unlike convection heat transfer via radiation can penetrate through solid barrier. Additionally, radiation can also be reflected by relatively high emissivity object which included glass shield, metal and water’s surface. Conduction heat transfer mode is also involved inside the distillation unit.

Energy balance is performed separately in each section of the distillation unit. As shown below, Eq. (3) represented energy balance of the insulator located at the bottom of the distillation unit.

$$m_{insul} C_{p.insul} \frac{dT_{insul.}}{dt} = I(t) A_{insul.} - q_{insul.} - q_{loss} \tag{3}$$

where q_{loss} is the amount of heat loss from system, $q_{insul.}$ is the amount of heat transferred from the insulator, $A_{insul.}$ is surface area of the insulator, $T_{insul.}$, $C_{p.insul.}$ is heat capacity of the insulator. An expanded polystyrene (EPS) with heat capacity of 1,300 J/(kg. K) was used as an insulator for this experiment because vapor cannot permeate through this insulator material. The weight of insulator ($m_{insul.}$) used was 2 kilograms.

The fourth equation described energy balance of the water surface in the bottom level of the distillation unit.

$$m_{H2O,1} C_{p,H2O} \frac{dT_{H2O,1}}{dt} = I(t) A_{H2O,1} + q_{insul} - q_{r,H2O,1} - q_{c,H2O,1} - q_{ev,H2O,1} \tag{4}$$

where $q_{r,H2O,1}$ is radiative heat transfer, $q_{c,H2O,1}$ is heat transfer via convection, $A_{H2O,1}$ is surface area $C_{p,H2O}$ or specific heat capacity of water is $4,178 \text{ J kg}^{-1} \text{ K}^{-1}$, $m_{H2O,1}$ is the mass of water inside the lower chamber, and $q_{ev,H2O,1}$ is heat transfer during evaporation.

Next Eq. (5) represented energy balancing of the transparent glass shield in the bottom chamber.

$$m_{gla,1} C_{p,gla,1} \frac{dT_{gla,1}}{dt} = I(t) A_{gla,1} + q_{r,gla,1} + q_{c,gla,1} + q_{ev,gla,1} - q_{c,gH1-2} \tag{5}$$

where $q_{c,gH1-2}$ is heat transfer between glass shield of the bottom chamber and water in the upper chamber, $T_{gla,1}$ is temperature monitored on the glass shield in the bottom chamber, $A_{gla,1}$ is surface area of glass shield in the bottom chamber, heat capacity of glass or $C_{p,gla,1}$ is equaled to $800 \text{ J kg}^{-1} \text{ K}^{-1}$, $m_{gla,1}$ is the weight of glass shield which is equaled to 5.7 kg.

Eq. (6) represent energy balance of the water body in the upper chamber.

$$m_{H2O,2} C_{p,H2O} \frac{dT_{H2O,2}}{dt} = I(t) A_{H2O,2} + q_{c,gH1-2} - q_{c,gH2-2} - q_{r,gH1-2} - q_{r,gH2-2} + q_{ABS} \tag{6}$$

where q_{ABS} is heat transfer from the heat absorber, $q_{c,gH1-2}/q_{r,gH1-2}$ is conductive/radiative heat transfer from glass shield in the bottom chamber to water body in the upper chamber, $q_{c,gH2-2}/q_{r,gH2-2}$ is conductive/radiative heat transfer from water body in the upper chamber to glass shield in the upper chamber, $A_{H2O,2}$ is surface area of the body of water.

Eq. (7) represented the energy balance of the glass shield in the upper chamber section of the distillation unit. Glass shield in this case was exposed to the atmosphere consisting of direct sunlight.

$$m_{gla,2} C_{p,gla,2} \frac{dT_{gla,2}}{dt} = I(t) A_{gla,2} + q_{c,gH2-2} + q_{r,gH2-2} + q_{ev,gH2-2} - q_{r,g2At} - q_{c,g2At} \tag{7}$$

where $q_{c,g2At}/q_{r,g2At}$ is heat transfer based on radiation mechanism between atmosphere, $A_{gla,2}$ is area of the glass shield in the upper chamber, $T_{gla,2}$ is the temperature measured at the glass shield in the upper chamber.

Eq. (8) demonstrated the collection of treated water in the form of distillation rate

$$\frac{dm_{DR}}{dt} = h_{e,gH1-1} \left[\frac{T_{H2O,1} - T_{gla,1}}{h_{fg@T_{H2O,1}}} \right] + h_{e,gH2-2} \left[\frac{T_{H2O,2} - T_{gla,2}}{h_{fg@T_{H2O,2}}} \right] \tag{8}$$

where $h_{e,gH1-1}/h_{e,gH2-2}/h_{fg@T_{H2O,1}}/h_{fg@T_{H2O,2}}$ are heat transfer coefficients used to as part of the differential equation and m_{DR} quantity of treated water collected at the bottom of the distillation unit.

2.3. Governing equation in the form of heat transfer in heat absorber

The equation below is used to find the quantity of energy that is transferred to the Titanium heat absorber.

$$q_{HA} = \alpha (I_{ab} \tau_{ab} + I_{rs} \tau_{rs}) \tag{9}$$

where τ_{rs} is defined as the directional movement of solar radiation with the flow of ununiformed steam, I_{rs} is defined as the solar radiation profile perpendicular to the impact area by hour, τ_{ab} is defined as the directional movement of solar radiation with the flow of absorbed steam and I_{ab} is defined as the solar radiation profile parallel the steam absorption vector and α is defined as the degree of absorption

2.4. Calculating the efficiency of solar distillation unit

Eq. (10) demonstrated the efficiency of the solar-based distillation unit.

$$\eta = \frac{\sum \dot{m}_d h_{fg}}{\sum I} \tag{10}$$

where I is summation of solar radiation derived daily, \dot{m}_d is the distillation rate based on the performance of distillation unit, and h_{fg} is latent heat.

2.5. Protocol for determining the distillation efficiency

Performance in terms of efficiency was calculated from operational input using the Engineer Equation Solver (EES). EES is a computer program used to mathematical find solution for complicated differential equations and multiple non-linear algebraic equations. Since many equations can be solving all at once. EES have been successfully use to give accurate transport properties of material and thermodynamic. Many add-on libraries were installed and used for the simulation in this research including heat transfer functions (conduction convection, and radiation), regression equation with uncertainty analysis module and graphical user input/output software features. Additional data such as the mechanical properties of the heat absorber (Titanium), solar radiation distribution functions, and rapid evaporation of high sodium chloride solution functions were added into the EES software with written Pascal codes. Fig. 1 illustrated the calculating logic and procedure used to command the EES. The first step is to find the value of solar radiation from Eq. (3) to Eq. (8). This can be done by plugging in the temperature at different location inside the distillation unit. Five sensor probes were installed inside the distillation unit to measure atmosphere temperature ($T_{at.}$), glass shield's temperature in the upper chamber ($T_{gla.2}$), water's temperature in the upper chamber ($T_{H2O.2}$) and glass shield's temperature in the bottom chamber ($T_{gla.1}$), water's temperature in the bottom chamber ($T_{H2O.1}$) and temperature of the insulator. According to the EES logic. Latent head was also employed to find the efficiency of the heat transfer system. Fig. 1 demonstrated various input parameters.

3. Methodology

3.1. Design of distillation system

This research developed a prototype distillation system with 2 slightly slanted water chambers as shown in Fig. 2. The unit is 100 cm x 150 cm x 65 cm. The water level in both chambers were initially set at 20 cm. The two covers were made out of transparent borosilicate glass with melting point of 400 °C. Multi-level platform was constructed from fiberglass material and coating with superhydrophobic paint in order to improve heat absorption and reduce fouling due to sodium chloride in salt water. The slope of both water chamber is controlled at 14°. Titanium metal sheet (grade 5 TA6V, 10 mm) was cut into various size block and then sanded using silicon carbide paper (240). Water solution for this experiment was prepared using NaCl 1M.

Various sensor was installed inside the distillation unit in order to record the temperature at different places in the unit. These data are combined with heat transfer coefficients, solar intensity measurements and water treatment rate in order to determine the efficiency of the system. The size of titanium heat absorber was also varied from 10% to 90% based on the surface area of glass shield on top of the upper chamber. K-type temperature sensors (Extech RHT20) were place to monitor water temperature, insulator temperature, and glass shield temperature. Initial amount of water in the bottom and upper chamber equaled to 24.6 liters and 75.2 liters. The amount of treated water that flow out of the outlet was measured using a volumetric flask. Wind speed was measured using an anemometer (Kestrel 0855YEL 5500 Weather Meter) attached to a digital data logger. Solar intensity was measured using the built-in solar light sensor with precision photo diode (Extech SP505). Conductivity of the water product was measured using a portable probe (Oakton CON 6+). The conductivity probe was used to confirm that water product no longer contain salt.

4. Results and discussion

4.1. Data acquisition for solar intensity

The distillation unit in this experiment were equipped with titanium heat absorber. Different size heat absorber as percentage of the glass shield surface area (10 to 90%) were used and compared. The distillation rate was also recorded by measuring the amount of treated water that flow out from the distillation unit. Solar intensity at the system installation were measured in the hottest month of the year which was in April 2019. Recorded data were analyzed and averaged to obtain a solar distribution profile. According to the collected data, as shown in Table 1, the average solar intensity was equaled to 413.54 W m⁻². The highest total solar intensity recorded at 13:00 was equaled to 912.5 W m⁻². Relative humidity corresponds well with the findings from solar intensity measurement. According to Table 1, the initial relative humidity recorded at 7:00 in the morning was 85.4%. An increase in solar intensity caused relative humidity to decrease to as low as 54.9% when measured at 15:00 in the afternoon. The weather condition during measurement of solar performance was mostly sunny with very little cloud.

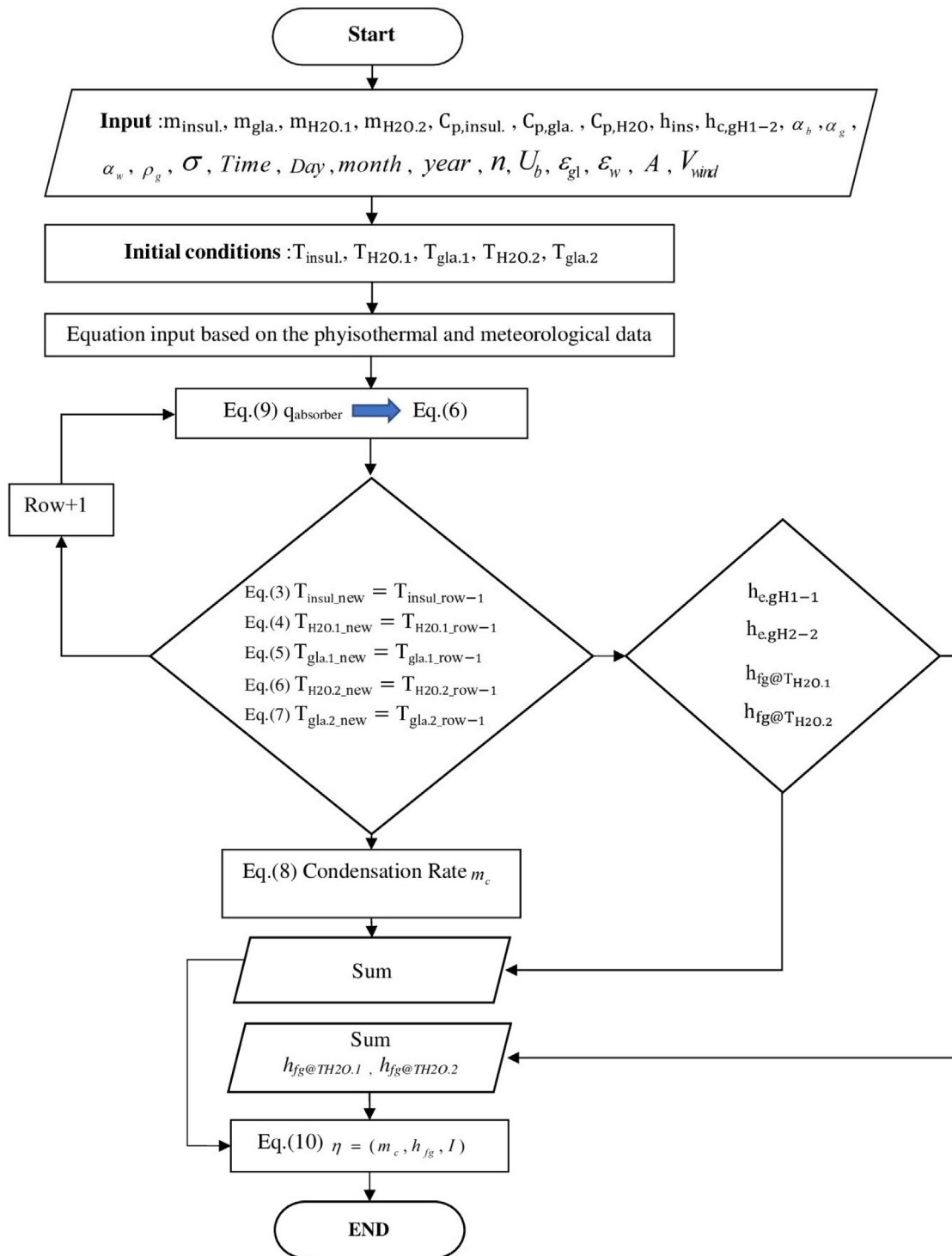


Fig. 1. Flow chart illustration of the logical path carried out by the Engineering Equation Solver (EES) to find efficiency.

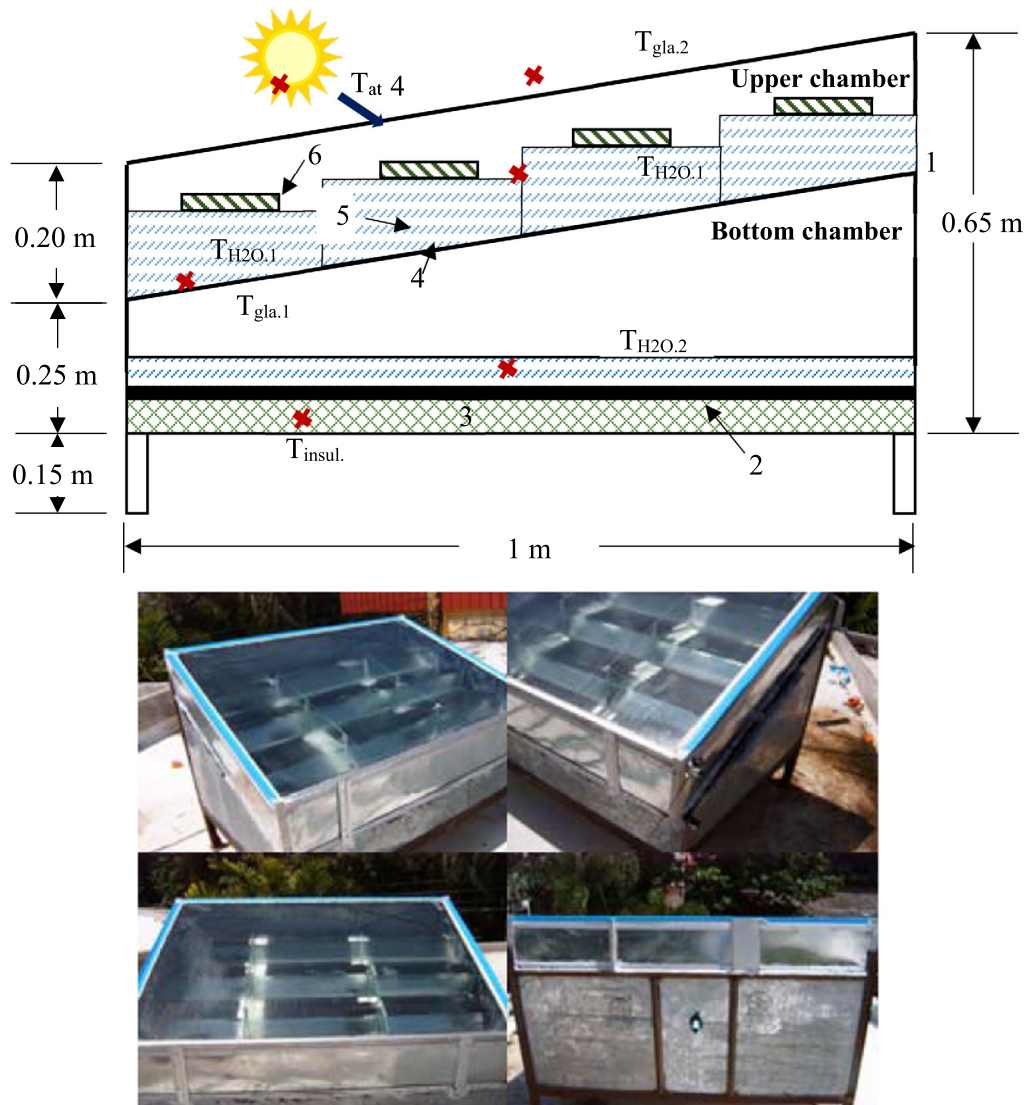


Fig. 2. Schematic diagram of the solar-based system. 1. Outlet, 2. Unit barrier wall, 3. Insulator, 4. Transparent glass cover, 5. Water channel/gutter, and 6. Heat absorber (red cross represent temperature probe locations).. (For interpretation of the references to color in this figure legend, the reader is referred to the web version of this article.)

4.2. Temperature profile monitor at different location inside the distillation unit

Distribution of temperature inside the solar-based system were analyzed from the averaged data. According to Fig. 3, maximum temperature measured from all of the sensor probe was recorded at 15:00 in the afternoon, which corresponded with very low humidity level. Insulator used in this experiments was made out of expanded polystyrene which have very effective heat control feature. For this reason, temperature recorded at the insulator was 54.6 °C, which was relatively the highest compared with temperature measured in other position. The lowest temperature inside the distillation unit was measured at glass shield. This is because glass have very low thermal conductivity. Therefore, heat transfer passed glass shield in form of radiation which does not increase temperature of the material. It is also observed that the water temperature measured in the bottom and upper chamber were significantly different. This gradient in temperature was found to promote heat transfer throughout the distillation unit. Additionally, it was observed that heat difference between glass shield and water depended significantly on whether the temperature was

Table 1. Average environmental condition measured throughout the day during the month of April 2019.

Time (hr)	Average solar intensity (w m^{-2})	Relative humidity (%)
7:00	14.2	85.4
8:00	144.3	83.1
9:00	321.3	82.8
10:00	623.3	78.3
11:00	785.5	70.1
12:00	875.9	62.6
13:00	912.5	56.2
14:00	632.3	55.8
15:00	370.6	54.9
16:00	218.6	67.4
17:00	47.0	72.1
18:00	17.0	78.9

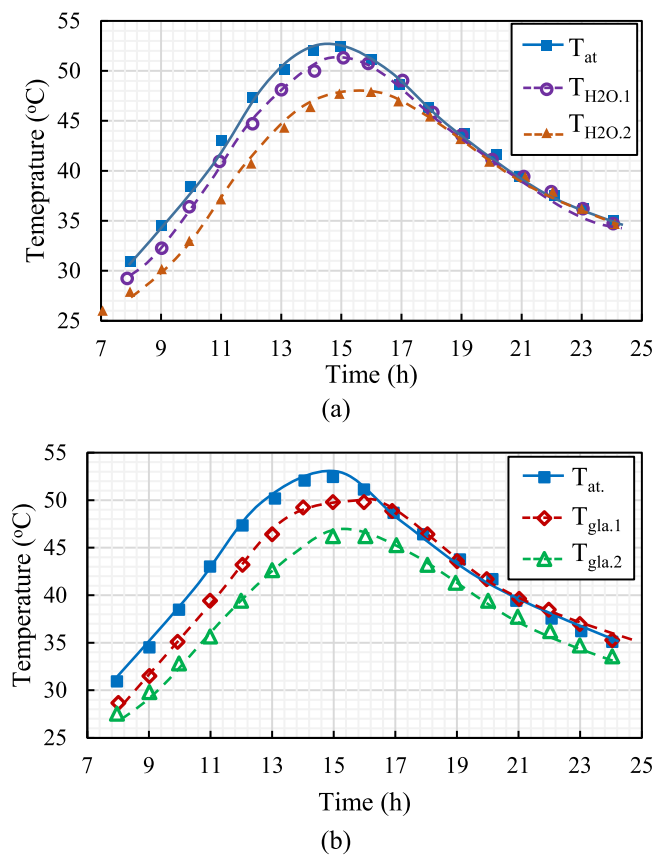


Fig. 3. Temperature measured at the upper and bottom chamber of (a) atmosphere–glass and (b) atmosphere–water system in distillation unit assisted by 10% size Titanium heat absorber.

measured in the upper or in the bottom chamber as shown in Fig. 4. This difference was even more recognition when measured was recorded after 10:00 in the morning. The largest temperature difference between water and glass shield was 6.93 °C in the upper chamber of the distillation unit. On the other hand, temperature difference measured at the bottom chamber was 6.12 °C.

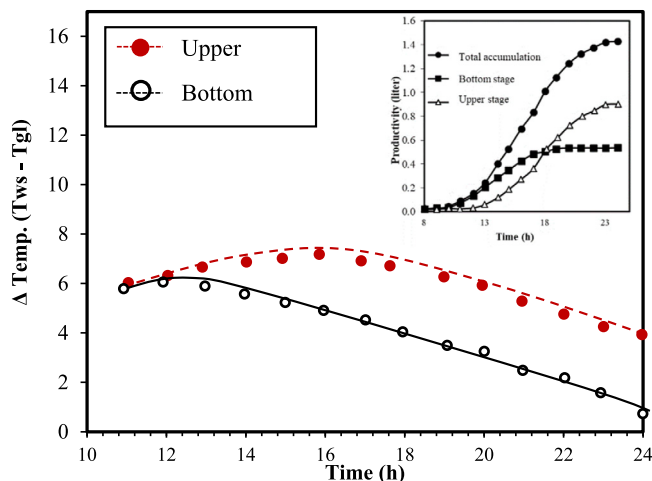


Fig. 4. Temperature difference between glass and water body in the upper and bottom chamber from 10:00 to 24:00 using distillation unit with 10% black gasket heat absorber (Inset: Accumulated productivity of water distillation in liters)..

4.3. Water treatment productivity and rate of distillation

The amount of distilled water collected after 10:00 in the morning to 24:00 at night is depicted in the inset of Fig. 4. Total accumulation of treated water was founded to be 1.52 liters. An increase in the rate of water treatment product can be observed from 10:00 to 16:00. This result corresponded with the atmospheric condition monitored simultaneously. Water treatment progress is slightly different between the bottom and the upper chamber. Distillation rate was calculated from the amount of water distilled throughout the experiment. As shown in Fig. 5, distillation rate in the bottom chamber was clearly lower than distillation rate calculated in the upper chamber. The reason behind this significant different in the distillation rate is the distinctive heat transfer gradient in the two chamber. The maximum distillation rate in the bottom and upper chamber was $0.007 \text{ g s}^{-1} \text{ m}^{-2}$ and $0.028 \text{ g s}^{-1} \text{ m}^{-2}$.

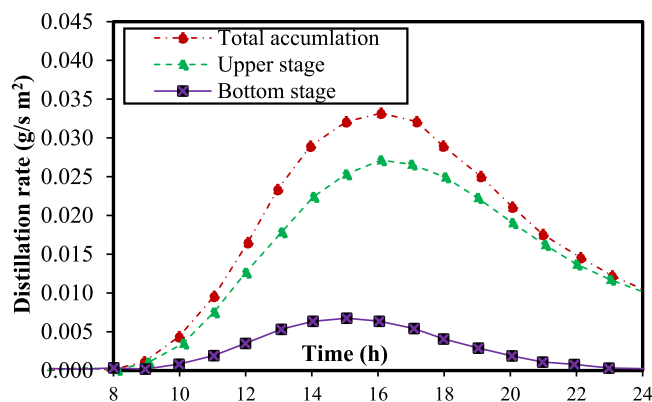


Fig. 5. Distillation rate calculated based on the period of time from 8:00 to 24:00.

In order to gain better understanding of the distillation performance in relation with the significant parameters two mathematical equation were derived. A polynomial model was used to predict the outcome of distillation process including productivity based on the size of heat absorber and productivity based on the distillation time interval. Eq. (11) demonstrated a polynomial model that can be used to predict efficiency of the distillation system as a function of the size of heat absorber.

Formation of the mathematical equation to predict productivity based on the period of time was also conducted. Among different mathematical models, polynomial model was found to sufficiently predict the outcome of the

experiment. As shown in Eq. (11), productivity (P_R) can be calculated as a function of operating time (OT_o) through the sixth order polynomial equation. Calculated value from Eq. (11) give very close productivity compared with the experimental data. Statistical analysis was revealed R^2 very closer to 1.

$$P_R = 4 \times 10^{-7}(OT_o)^6 - 3 \times 10^{-5}(OT_o)^5 + 0.0009(OT_o)^4 - 0.0092(OT_o)^3 + 0.0521t_o^2 - 0.1125t_o + 0.1120 \quad (11)$$

Influence of wind speed on the distillation rate was illustrated in Fig. 6. During the course of the experiment different wind speed was measured from 1 m s^{-1} to 10 m s^{-1} . Distillation rate was observed to increase with wind speed. Additionally, it was also found that the distillation rate decreased with water height and thermal conductivity of the insulator as shown in Fig. 7. Water height influence distillation rate because water height is a barrier which shielded sunlight from heat absorber. Thermal conductivity of the insulator was modified by addition of silicon carbide. On the other hand, an increase in thermal conductivity of Titanium heat absorber was found to cause distillation rate to increase.

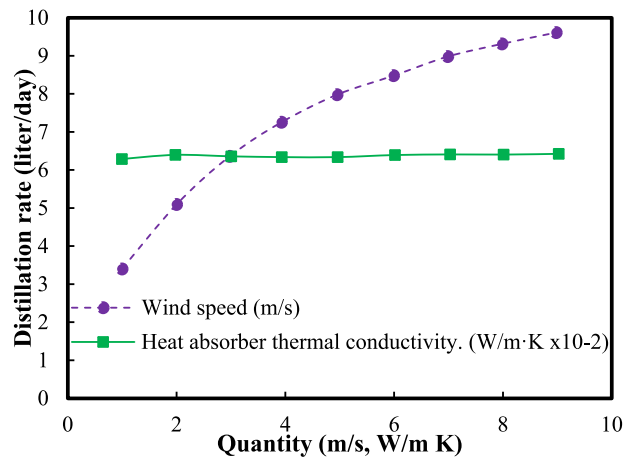


Fig. 6. Effect of wind speed and heat absorber thermal conductivity on the distillation rate of the system.

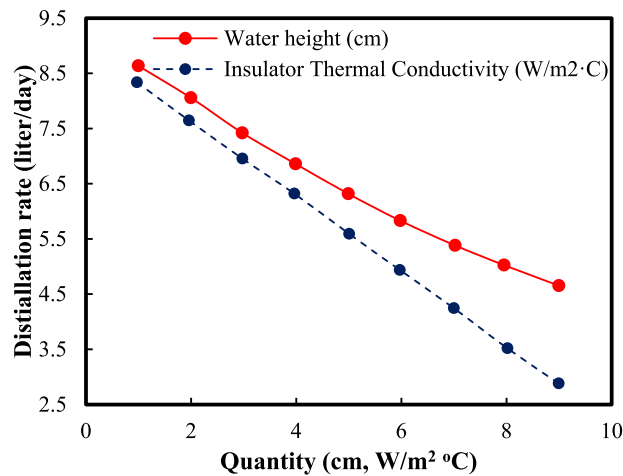


Fig. 7. Influence of water height and thermal conductivity of insulator on distillation rate.

The relationship between heat absorber’s size and efficiency can be demonstrated in Eq. (12), which is a fourth order polynomial. Statistical analysis between experimental and mathematical model revealed R^2 of 0.9985. Eq. (12) was proposed as a function of heat absorber size (a_H). Relationship between size of heat absorber and distillation

efficiency is shown in Fig. 8.

$$\text{Efficiency}(\%) = 9.7611 \times 10^{-7}(A_H)^4 - 0.0002(A_H)^3 + 0.0104(A_H)^2 - 0.3292(A_H) + 28.3291 \quad (12)$$

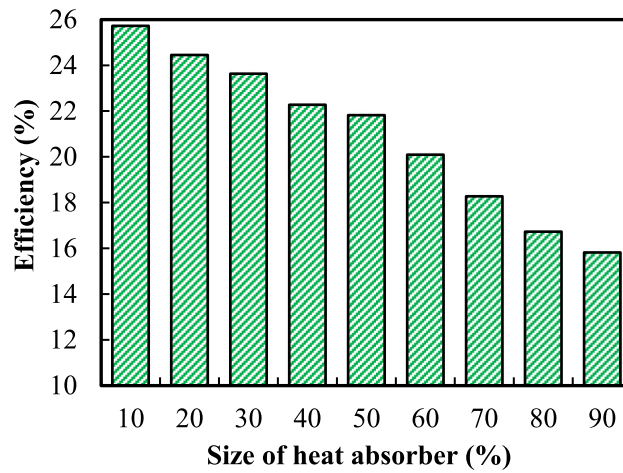


Fig. 8. Influence of size of heat absorber on the efficiency of the distillation system.

Efficiency and productivity of the distillation unit assisted by different type of heat absorber were illustrated in Fig. 9. It is clearly observed that Aluminum performed significantly better than other metal follow by Titanium heat absorber. Other heat absorber such as black gasket, rubber and zinc demonstrated similar efficiency and productivity. Maximum capacity of the distillation unit can be calculate from the productivity of the prototype distillation unit. The productivity will be linearly proportional to the effective volume of the distillation unit.

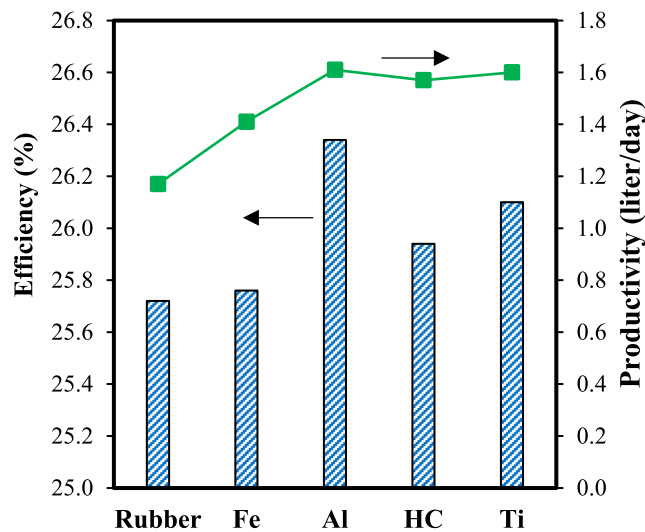


Fig. 9. Comparison between efficiency and productivity of distillation unit with different type of heat absorbers (Fe = black iron gasket, Al = aluminum, HC = High carbon steel, and Ti = Titanium).

4.4. Economic analysis of solar-based distillation system

Economic analysis of the prototype solar-based distillation system can be performing based on input data including payback period after investment and the total cost of distillation activity. The total cost of distillation

process for water treatment system (TC_{dist}) is subject to the yearly interest rate (i), capital cost of the water chambers (C_{wc}), the anticipated lifetime of the prototype (N_{year}), value of solar-based system after anticipated lifetime (V_{end}), yearly productivity (P_{year}), yearly operating and maintenance cost (OM_c). The price of land for equipment installation, tax rate, insurance and price of salt water is not part of the analysis. The maintenance cost comprises of yearly cost required to eliminated salt deposited at the bottom of the water chamber, to clean the transparent glass cover, and daily water replacement inside the chamber due to water loss. Table 2 demonstrated the input parameters used for the feasibility analysis. The variation of productivity is linearly proportional to the dimension of the distillation unit.

Table 2. Payback period of solar-based distillation prototype using different type of heat absorber.

Conditions	Values
OM_c	10% of the yearly capital cost of the solar-based prototype
C_{wc}	5,000 Baht per m^2 for the construction of solar-based distillation system in Thailand
N_{year}	8
i	7
V_{end}	5% of the capital cost of the solar-based prototype
P_{year}	Titanium = 584 liter/year, high carbon = 576.7 liter/year, aluminum = 591.3 liter/year, iron = 511 liter/year, and black rubber= 408.8 liter/year

The value of specific cost of water treatment (SC_{water}) using the prototype is calculated based on the ratio between total yearly costs of the chamber (TC_{year}) and the yearly productivity as shown in equation below.

$$SC_{water} = \frac{\text{Total yearly cost of the chamber}}{P_{year}} \tag{13}$$

The total yearly cost of the chamber (TC_{year}) in the distillation system can be calculated using the equation below.

$$TC_{year} = YC_{wc} + OM_c - YV_{end} \tag{14}$$

Where YC_{wc} is the yearly cost of the water chamber, OM_c is operating maintenance cost and YV_{end} is the yearly value of solar-based system after anticipated lifetime.

The payback period (P_{period}) of the distillation system is calculated by taking into account the cash flow (C_{flow}) of the project, capital and interest rate as shown in the equation below.

$$P_{period} = \frac{\ln \left[\frac{C_{flow}}{C_{flow} - (C_{wc} \times i)} \right]}{\ln [1 + i]} \tag{15}$$

Cash flow of the water treatment system can be found using the equation below.

$$C_{flow} = P_{year} \times WP \tag{16}$$

Where WP is the price of the water that was treated by the prototype solar distillation system.

The payback period calculated from economic analysis of the prototype was 5.5 years when titanium was used as heat absorber were illustrated in Fig. 10.

4.5. Feedback on design and usability from user

Prior to building the distillation system, researchers gather information on customer’s requirements in order to really understand what userñ in the area wanted. This was conducted by both face-to-face interview and filling of survey questionnaire. From these interview and surveys, it was found that the important criteria for the design of distillation system consisted of weight of system, degree of mobility, cost of system and durability. After construction and testing of the distillation system in different areas it was found that most users gave positive feedback on the

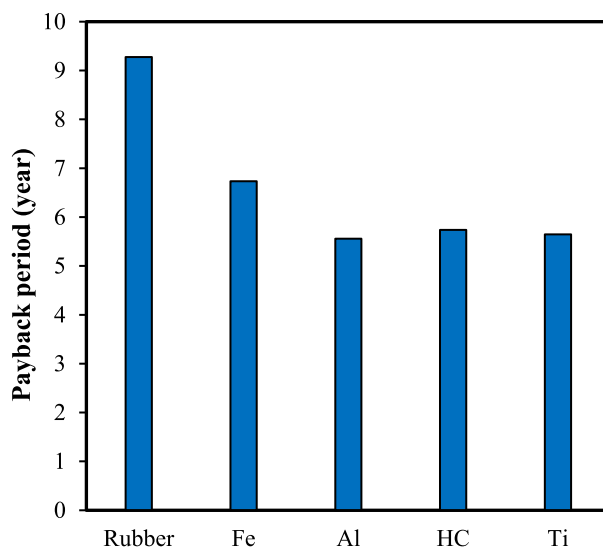


Fig. 10. Comparison of payback period for each type of heat absorber (Fe = black iron gasket, Al = aluminum, HC = High carbon steel, and Ti = Titanium).

four main criteria. Three out of four establishments decided to scale-up the prototype to increase the capacity output of the distillation system. However, one of the establishment decided to use aluminum instead of titanium because the place of titanium material is quite expensive. The current capacity of the distillation system is 408.8 to 591.3 liter per year depending on the type of heat absorber. An increase in capacity of the distillation can be achieved by expanding the upper and lower water compartment. In order to minimize the negative impact, it is possible to change the shape of the heat absorber and add nanoparticle coating on the surface of the heat absorber.

5. Conclusion

This research developed an appropriate prototype for water treatment using solar radiation to perform water vaporization. The surface area of heat absorber was found to have a negative impact on the efficiency of the prototype distillation unit. The amount of treated water reached 1.61 liter per day at an efficiency of 26.2% when the prototype was operated under the optimum circumstance. The payback period calculated from economic analysis of the prototype was 5.5 years when titanium was used as heat absorber.

Distillation rate peaked around 15:00 at $0.028 \text{ g s}^{-1} \text{ m}^{-2}$ combining the productivity of both the bottom and upper chamber. External factor such as wind speed and thermal conductivity of the heat absorber was found to have positive effect on the efficiency of the prototype. In contrary, insulator's thermal conductivity and water height have a negative impact on efficiency. Experimental data were fitted using polynomial equation, which can be used to predict efficiency and water treatment productivity. Both equation was statically very close to the actual experiment data. Comparison between different type of heat absorber were illustrated. Aluminum was observed to have the highest efficiency and productivity followed by Titanium. Feedback from local user indicated successful design parameters and cost effective investment opportunity.

Declaration of competing interest

The authors declare that they have no known competing financial interests or personal relationships that could have appeared to influence the work reported in this paper.

Acknowledgments

This study was supported by the Program Management Unit for Human Resources & Institutional Development, Research and Innovation, NXPO (grant number B05F630092) and Thailand Science Research and Innovation Fundamental Fund (Project No. 66082). Also special thanks to Kriengkrai Nabudda's research group for assisting with the experiment and data collections.

References

- [1] Kampf G, Todt D, Pfaender S, Steinmann E. Persistence of coronaviruses on inanimate surfaces and their inactivation with biocidal agents. *J Hosp Infect* 2020;104(3):246–51.
- [2] Wang XW, Li J-S, Jin M, Zhen B, Kong QX, Song N, et al. Study on the resistance of severe acute respiratory syndrome-associated coronavirus. *J Virol Methods* 2005;126(1):171–7.
- [3] Cao Y, Wang Q, Niu B. Potential of solar heating for ultra-low-energy passive buildings in cold regions. *Int J Heat Technol* 2019;37(4):1052–8.
- [4] Nimnuan P, Janjai S. An approach for estimating average daily global solar radiation from cloud cover in Thailand. *Procedia Eng* 2012;32:399–406.
- [5] McNeil N, Musikasuwan S, Bright E, Owusu B. Statistical analysis of solar radiation in southern Thailand. *Nature Environ Pollut Technol* 2019;18:543–8.
- [6] Global solar atlas. Solar resource and PV power potential maps and GIS from <https://globalsolaratlas.info/downloads/thailand>. 2016.
- [7] Jamroen C, Komkum P, Kohsri S, Himananto W, Panupintu S, Unkat S. A low-cost dual-axis solar tracking system based on digital logic design: Design and implementation. *Sustain Energy Technol Assess* 2020;37:100618.
- [8] Mohajeri N, Gudmundsson A, Kunckler T, Upadhyay G, Assouline D, Kämpf JH, Scartezzini JL. A solar-based sustainable urban design: The effects of city-scale street-canyon geometry on solar access in Geneva, Switzerland. *Appl Energy* 2019;240:173–90.
- [9] Mohajeri N, Upadhyay G, Gudmundsson A, Assouline D, Kämpf J, Scartezzini J-L. Effects of urban compactness on solar energy potential. *Renew Energy* 2016;93:469–82.
- [10] Sampathkumar K, TVA, Pitchandi P, Senthilkumar P. Active solar distillation—A detailed review. *Renew Sustain Energy Rev* 2010;14:1503–26.
- [11] Hosseini A, Banakar A, Gorjian S. Development and performance evaluation of an active solar distillation system integrated with a vacuum-type heat exchanger. *Desalination* 2018;435:45–59.
- [12] Pannucharoenwong N, Rattanadecho P, Echaroj S, Hemathulin S, Nabudda K. The experiment of heat absorber from black gasket on the efficiency of double slope solar still. *GMSARN Int J* 2020;14(1):1–10.
- [13] Pannucharoenwong N, Rattanadecho P, Echaroj S, Nabudda K. Investigation of double slope solar distillation efficiency using heat absorber made from zinc. *Sci Technol Asia* 2019;24(4):70–82.
- [14] Ranjbaran A, Norozi M. Design and fabrication of a novel hybrid solar distillation system with the ability to brine recycling. *Int J Heat Technol* 2018;37(3):751–60.
- [15] Sharshir SW, Ellakany YM, Algazzar AM, Elsheikh AH, Elkadeem MR, Edreis EMA, et al. A mini review of techniques used to improve the tubular solar still performance for solar water desalination. *Process Saf Environ Prot* 2019.
- [16] Kumar BS, Kumar S, Jayaprakash R. Performance analysis of a “V” type solar still using a charcoal absorber and a boosting mirror. *Desalination* 2008;229(1):217–30.
- [17] Mona N Radwan, Morad MM, Ali MM, Kamal I Wasfy. A solar steam distillation system for extracting lavender volatile oil. *Energy Rep* 2020;6:3080–7.
- [18] Ahmad K, Sleiti, Wahib A, Al-Ammari, Al-Khawaja Mohammed. Integrated novel solar distillation and solar single-effect absorption systems. *Desalination* 2021;(507):115032.